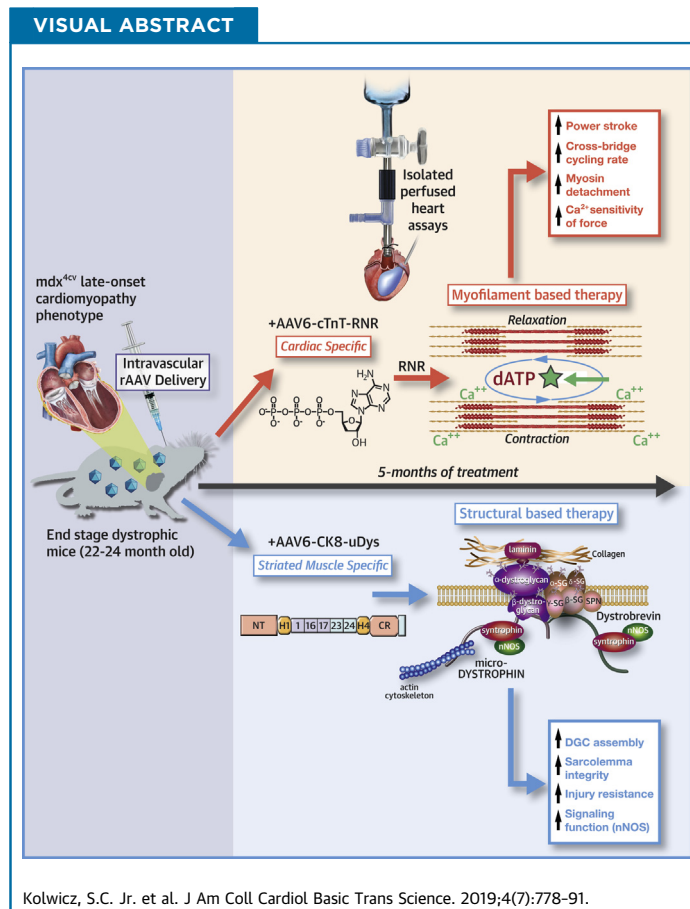


PRECLINICAL RESEARCH

Gene Therapy Rescues Cardiac Dysfunction in Duchenne Muscular Dystrophy Mice by Elevating Cardiomyocyte Deoxy-Adenosine Triphosphate



Stephen C. Kolwicz, Jr, PhD,^a John K. Hall, PhD,^b Farid Moussavi-Harami, MD,^c Xiolan Chen, PhD,^{d,e}
Stephen D. Hauschka, PhD,^{d,e} Jeffrey S. Chamberlain, PhD,^{b,d,e} Michael Regnier, PhD,^{e,f,g,*} Guy L. Odom, PhD^{b,e,g,*}



HIGHLIGHTS

- rAAV vectors increase cardiac-specific expression of RNR and elevate cardiomyocyte 2-dATP levels.
- Elevated myocardial RNR and subsequent increase in 2-dATP rescues the performance of failing myocardium, an effect that persists long term.

- We show the ability to increase both cardiac baseline function and high workload contractile performance in aged (22- to 24-month old) *mdx4cv* mice, by high-level muscle-specific expression of either microdystrophin or RNR.
- Five months post-treatment, mice systemically injected with rAAV6 vector carrying a striated muscle-specific regulatory cassette driving expression of microdystrophin in both skeletal and cardiac muscle, exhibited the greatest effect on systolic function. In comparison, mice treated with rAAV6 vector carrying RNR that expresses exclusively in cardiac muscle not only exhibited greatly improved baseline systolic function but also improved diastolic function.
- Importantly, vector-directed overexpression of RNR did not impair cardiac reserve during increased physiological demand in aged *mdx4cv* hearts.

SUMMARY

Mutations in the gene encoding for dystrophin leads to structural and functional deterioration of cardiomyocytes and is a hallmark of cardiomyopathy in Duchenne muscular dystrophy (DMD) patients. Administration of recombinant adeno-associated viral vectors delivering microdystrophin or ribonucleotide reductase (RNR), under muscle-specific regulatory control, rescues both baseline and high workload-challenged hearts in an aged, DMD mouse model. However, only RNR treatments improved both systolic and diastolic function under those conditions. Cardiac-specific recombinant adeno-associated viral treatment of RNR holds therapeutic promise for improvement of cardiomyopathy in DMD patients. (J Am Coll Cardiol Basic Trans Science 2019;4:778-91) © 2019 The Authors. Published by Elsevier on behalf of the American College of Cardiology Foundation. This is an open access article under the CC BY-NC-ND license (<http://creativecommons.org/licenses/by-nc-nd/4.0/>).

ABBREVIATIONS AND ACRONYMS

μDys = microdystrophin
CK8 = miniaturized murine creatine kinase regulatory cassette
CMV = cytomegalovirus
cTnT = cardiac troponin T
dADP = deoxy-adenosine diphosphate
dATP = deoxy-adenosine triphosphate
DMD = Duchenne muscular dystrophy
mdx = mouse muscular dystrophy model
rAAV = recombinant adeno-associated viral vector
RNR = ribonucleotide reductase

Duchenne muscular dystrophy (DMD) and its milder and allelic form, Becker muscular dystrophy (BMD), are the most frequent muscular dystrophies, occurring once in ~5,000 male births, and are due to mutations in the dystrophin gene (1). DMD patients typically die due to cardiac and respiratory muscle failure; thus, maintenance of adequate function in both cardiac and skeletal muscle is critical for optimal DMD therapy. The primary function of dystrophin is to provide a structural role by mechanically linking the subsarcolemmal cytoskeleton to the extracellular matrix through the dystrophin-glycoprotein complex (DGC) (2). This linkage transmits the forces of contraction to the extracellular matrix and protects muscles

from contraction-induced injury (3-7). In addition to a structural or mechanical role, the DGC also serves as a scaffold for cytoplasmic and membrane-associated signaling proteins and ion channels (8-11). The complete absence of dystrophin results in drastic reductions of all DGC components (12-14). Together, an absence of dystrophin and reduction in the DGC components causes membrane destabilization and permeability defects that lead to myofiber degeneration, repeated cycles of degeneration/regeneration, and the gradual replacement of muscle fibers with fibrotic, connective, and adipose tissue.

In contrast, some in-frame deletions, truncations, and missense mutations lead to reduced dystrophin expression associated with milder phenotypes. These

From the ^aMitochondria and Metabolism Center, University of Washington, Seattle, Washington; ^bDepartment of Neurology, University of Washington, Seattle, Washington; ^cDivision of Cardiology, Department of Medicine, University of Washington, Seattle, Washington; ^dDepartment of Biochemistry, University of Washington, Seattle, Washington; ^eWellstone Muscular Dystrophy Specialized Research Center, University of Washington, Seattle, Washington; ^fDepartment of Bioengineering, University of Washington, Seattle, Washington; and the ^gCenter for Cardiovascular Biology, University of Washington, Seattle, Washington. *Drs. Regnier and Odom contributed equally to this work and are joint senior authors. This work was supported by grants from the National Institutes of Health (NIH): R01 HL111197 (to Dr. Regnier and Hauschka), R01 HD048895, K08 HL128826 (to Dr. Moussavi-Harami) and R01 HL128368 (to Dr. Regnier) and 1U54AR065139-01A1 (to Drs. Hauschka, Chamberlain, Regnier, and Odom). Dr. Kolwicz was funded by the American Heart Association 14SDG18590020. Dr. Chamberlain has received personal fees from Solid Biosciences, SAB. All other authors have reported that they have no relationships relevant to the contents of this paper to disclose.

The authors attest they are in compliance with human studies committees and animal welfare regulations of the authors' institutions and US Food and Drug Administration guidelines, including patient consent where appropriate. For more information, visit the *JACC: Basic to Translational Science* [author instructions page](#).

Manuscript received February 27, 2019; revised manuscript received June 20, 2019, accepted June 20, 2019.

pathologies are largely curtailed in mouse (*mdx*) and canine (*cxmd*) models of DMD following the vector-mediated delivery of muscle-specific expression of highly functional miniaturized versions of dystrophin, microdystrophin (μ Dys) (15-24). In *mdx* mice, muscle pathology is milder than in humans, with the exception of the diaphragm; however, the dystrophic phenotype worsens with increasing age including the development of cardiac dysfunction (25-32). Administration of recombinant adeno-associated viral (rAAV)-mediated μ Dys therapy in *mdx* mice preceding the onset of cardiomyopathy is highly cardioprotective (33-35). However, when *mdx* mice are treated with μ Dys at a late stage of cardiomyopathy, such as would be the case for a number of DMD patients, a full rescue of the dysfunctional cardiac phenotype is not achieved (30,35-37).

SEE PAGE 792

We have developed a cardiac function-enhancing gene therapy approach that targets myosin in contractile filaments by overexpressing the enzyme ribonucleotide reductase (RNR). RNR converts adenosine diphosphate (ADP) to deoxy-ADP (dADP), which is rapidly converted to deoxy-adenosine triphosphate (dATP) in cells. In numerous in vitro studies, we have shown that dATP increases cross-bridge binding and cycling, resulting in stronger, faster contraction and faster relaxation (38-45). We have also reported that dATP improves contractile properties of myocardium from end-stage human heart failure (HF) in vitro (42) and dogs with end-stage idiopathic dilated cardiomyopathy (46). In normal rodent muscle, we reported that increases in cardiomyocytes and cardiac function occur with as little as ~1% of the ATP pool in the dATP form (40,47). Similarly, rAAV-mediated delivery of RNR under cardiac-specific regulatory control resulted in enzyme overexpression exclusively in cardiomyocytes and significantly improved left ventricular function without adverse cardiac remodeling in normal and infarcted rodent hearts (48). Our data indicated that dATP could rescue the preload responsiveness of failing hearts, suggesting restoration of the abnormal Frank-Starling Law of the Heart that often occurs in HF.

In the current study, we compare the relative therapeutic capacity of CK8-driven μ Dys or cardiac troponin T (cTnT)-driven RNR, via intravenously administered rAAV vectors in an advanced-age, DMD cardiomyopathy mouse model. We show a restoration of myocardial workload as indicated by rate pressure product (RPP) for baseline function in *mdx*^{4cv} mice treated with RNR. This outcome was primarily attributed to the normalization of left ventricular

developed pressure (LVDevP). Although *mdx*^{4cv} mice treated with μ Dys appeared to normalize LVDevP, this did not result in a significant increase in RPP. Upon further evaluation of cardiac function, the pressure-volume relationship revealed that systolic pressure response with increased preload was significantly improved with the treatment of either RNR or μ Dys. However, only RNR treatment resulted in significant improvements in diastolic functional parameters, returning them to values that were similar to wild-type (WT) control hearts. As a further assessment of cardiac function, we tested hearts using a high workload challenge protocol. Both RNR and μ Dys treatments improved systolic function in *mdx*^{4cv} hearts without compromising cardiac reserve. These positive results suggest that targeted expression of RNR within the myocardium can significantly improve contractile performance in an advanced-age model of DMD cardiomyopathy and may have therapeutic implications for DMD patients.

METHODS

ANIMAL EXPERIMENTS. Male WT C57Bl/6J (The Jackson Laboratory, Bar Harbor, Maine) and *mdx*^{4cv} (generated in-house) mice were used for these studies (17). All animals were experimentally manipulated in accordance with the Institutional Animal Care and Use Committee of the University of Washington. Experimental mice were administered vector at 22 to 24 months of age via the retro-orbital sinus with a 200- μ l bolus injection in Hanks balanced saline solution at a dose of 2×10^{14} vg/kg. All mice were housed in a specific-pathogen free animal care facility using a 12-h light/12-h dark cycle with access to food and water ad libitum.

VECTOR PRODUCTION. rAAV genomes containing the CK8 regulatory cassette (expressed exclusively in skeletal and cardiac muscle) and the human codon optimized (GenScript) μ Dys (Δ R2-15/ Δ R18-22/ Δ CT) (24), followed by the rabbit beta-globin poly-adenylation (pA) signal, were generated using standard cloning techniques. The rAAV genomes containing the cardiac muscle-specific cTnT455 regulatory cassette, the codon optimized human RNR transgene flanked by 100-bp untranslated regions, and the rabbit beta-globin pA were generated as previously described (48). The “dead” rAAV genomes or promoter-less firefly luciferase followed by the human growth hormone (hGH) pA (kindly provided by J.S.C., University of Washington, Seattle, Washington) were used to generate the control rAAV genomes. The resulting constructs were cotransfected with the pDG6 packaging plasmid into HEK293 cells to

generate rAAV vectors carrying serotype 6 capsids, which were harvested, enriched, and quantitated as previously described (49).

VECTOR GENOME QUANTIFICATION. Total DNA was extracted from flash-frozen tissue samples with Tri-Reagent (MRC Inc., Cincinnati, Ohio), according to manufacturer's instructions. All real-time polymerase chain reaction (PCR) reactions were performed on a QuantStudio 3 Real Time PCR System (Applied Biosystems, Foster City, California) in a total volume of 15 μ l, consisting of 5 μ l sample DNA, 10.0 μ l TaqMan Universal PCR Master Mix (Applied Biosystems), 0.2 μ M of each primer, and 0.1 μ M TaqMan custom probe (Applied Biosystems). Reaction conditions were 50° C for 2 min, 95° C for 10 min, and 40 cycles of [95° C for 15 s followed by 60° C for 1 min]. Each sample was analyzed in triplicate for concentration of total murine genomes and of total vector genomes. For vector genome detection by quantitative PCR, the primers used to amplify either the rAAV6-cTnT455-RNR or rAAV6-CK8- μ Dys, or rAAV6- Δ cytomegalovirus(CMV)-Luc (control vector) were unique to each vector. For the RNR vector, the amplicon spanned from the distal region of the cTnT promoter, continuing into the proximal RNR1 subunit. For the μ Dys vector, the amplicon was contained within the CK8 regulatory cassette, whereas the amplicon for the control vector resided within the hGH pA. hGH primers included: 5'-CACAACTCTGGCTCACTGCAA-3', 5'-GGAGGCTGAGGCAGGAGAA-3'; TaqMan probe: 5'-6FAM-CTCCGCC TCCTGGGTTCAAGCG-MBGNQ-3'; CK8 RC primers: 5'-CCCGAGATGCCTGGTTATAATT-3', 5'-CGGGAACATGGCATGCA-3'; TaqMan probe: 5'-6FAM-CCCCCAACACCTGCTGCCTCT-MBGNQ-3'; cTnT455-RNR1 primers: 5'-CCCAGTCCCCGCTGAGA-3', 5'-AGGTCCAGGCGCTGCT-3'; and TaqMan probe: 5'-6FAM-ACTCATCAATGTATCTTATCATG-MBGNQ-3'. Results were presented relative to DNA content in each 5- μ l DNA tissue sample to determine vector genomes per ng DNA.

TISSUE PROCESSING AND IMAGING ANALYSIS. Tissues were collected and analyzed 5 months post-administration of vectors and compared with age-matched male control vector (rAAV6- Δ CMV-Luc) injected *mdx*^{4cv} and WT mice. Hearts were either snap frozen in liquid nitrogen or were embedded in optimal cutting temperature compound (VWR International, Bridgeport, New Jersey) and flash frozen in liquid nitrogen cooled isopentane for histochemical or immunofluorescence analysis. The snap frozen samples were further processed by grinding to a powder under liquid nitrogen in a mortar kept on dry ice for subsequent extraction of nucleic acid and protein.

Heart cross-sections (10 μ m) were co-stained with antibodies raised against alpha 2-laminin (Sigma, St. Louis, Missouri; rat monoclonal, 1:200), the hinge-1 domain of dystrophin (alexa488 conjugated MAN-EX1011b, Developmental Studies Hybridoma Bank, University of Iowa, mouse monoclonal, 1:200), the human RRM1 (Abcam, Cambridge, United Kingdom; rabbit monoclonal, 1:200), and the human RRM2 (Abcam, rabbit monoclonal, 1:200). Conjugated secondary antibodies (Jackson Immuno, Goat anti-Rabbit) were used at a 1:500 dilution. Slides were mounted using ProLong Gold with DAPI (Thermo Fisher Scientific) and imaged via a Leica SPV confocal microscope. Confocal micrographs covering a majority of the heart left ventricular muscle sections were acquired and montaged via the Fiji toolset (ImageJ) and InDesign (Adobe, San Jose, California). For histology, Masson's trichrome staining was used to examine heart cross-sections. Briefly, 10- μ m muscle cryosections were sequentially stained in Wiegert's iron hematoxylin (10 min), 1% Ponceau-acetic acid (5 min), and 1% aniline blue (5 s).

WESTERN BLOTTING. Radioimmunoprecipitation analysis buffer supplemented with 5 mM ethylenediaminetetraacetic acid and 3% protease inhibitor cocktail (Sigma, Cat# P8340), was used to extract muscle proteins for 0.5 h on ice with gentle agitation every 10 min. Total protein concentration was determined using Pierce BCA assay kit (Fisher Scientific, Kent, Washington). Muscle lysates from WT, control *mdx*^{4cv}, and treated *mdx*^{4cv} (30 μ g) mice were denatured at 99°C for 10 min, quenched on ice, and separated via gel electrophoresis after loading onto Criterion 4-12% Bis-Tris polyacrylamide gels (BioRad). Overnight protein transfer to 0.45 mm polyvinylidene difluoride membranes was performed at constant 43 volts at 4°C in Towbin's buffer containing 20% methanol. Blots were blocked for 1 h at room temperature in 5% non-fat dry milk for 1 h before overnight incubation with antibodies raised against the hinge-1 region of dystrophin (Developmental Studies Hybridoma Bank, University of Iowa, 1:300), anti-RRM1 (Abcam, rabbit monoclonal, 1:1,000), anti-RRM2 (Abcam, rabbit monoclonal 1:1,000), and anti-GAPDH (Sigma, Rabbit polyclonal, 1:50,000). Horseradish-peroxidase conjugated secondary antibody staining (1:50,000) was performed for 1 h at room temperature before signal development using Clarity Western ECL substrate (BioRad) and visualization using a Chemidoc MP imaging system (BioRad).

QUANTIFICATION OF CARDIAC dATP. Approximately 25 μ g of flash frozen, freshly ground ventricle

cardiac tissue was used for direct quantification of intracellular dATP using the high-performance liquid chromatography (HPLC)-with tandem mass spectrometry (MS/MS) method previously described (50). Briefly, samples were extracted 1 to 3 days before measurement using a 50% methanol solution. The supernatant was stored at -20°C until ready for injection into the HPLC-MS/MS system. A Waters Xevo-TQ-S mass spectrometer coupled with a Waters Acquity I-Class HPLC was used for the analysis (Milford, Massachusetts). Monitoring in negative mode via electrospray ionization was used to acquire MS/MS ions. dATP concentrations were quantified with standards and normalized to tissue weight.

LANGENDORFF ISOLATED PERFUSED HEART EXPERIMENTS. Ex vivo cardiac function was assessed in Langendorff isolated heart preparations as previously described (47,48,51). Hearts were perfused at a constant pressure of 80 mm Hg with a modified Krebs-Henseleit buffer supplemented with glucose and pyruvate. The perfusate contained (mmol/l): 118 NaCl, 25 NaHCO₃, 5.3 KCl, 2.0 CaCl₂, 1.2 MgSO₄, 0.5 ethylenediaminetetraacetic acid, 10.0 glucose, and 0.5 pyruvate, equilibrated with 95% O₂ and 5% CO₂ (pH 7.4). Temperature was maintained at 37.5°C throughout the protocol. Left ventricular (LV) function was monitored via a water-filled balloon inserted into the LV and connected to a pressure transducer. LV systolic pressure (LVSP), end diastolic pressure, heart rate (HR), and minimum and maximum rate of pressure change in the ventricle (\pm dP/dt) were obtained from the attached data acquisition system (PowerLab, ADInstruments, Colorado Springs, Colorado). After 5 min of stabilization, hearts were equilibrated for 10 min at spontaneous HRs and then fixed at a HR of ~450 beats/min with an electrical stimulator (Grass Technologies, Warwick, Rhode Island). Pressure-volume relationships (i.e., Frank-Starling curves) were assessed by gradually increasing the volume of the LV balloon. After a 5-min recovery period, the perfusate was changed to an identical buffer as above except for the addition of 4.0 mmol/l CaCl₂ to simulate a high workload challenge for 20 min.

STATISTICAL ANALYSIS. All values are reported as means \pm SEM. Starling curves and high workload function were analyzed by 2-way repeated measures analysis of variance followed by pairwise comparisons using Tukey's alpha adjustment method. Other endpoint data were analyzed via 1-way analysis of variance or Student's *t*-tests as appropriate. Kaplan-Meier methods were used to analyze survival curves and compared using the log-rank test. Statistical

significance was tested at the $p < 0.05$ level. Statistical analyses were completed using Prism 7.0 (GraphPad Software, San Diego, California).

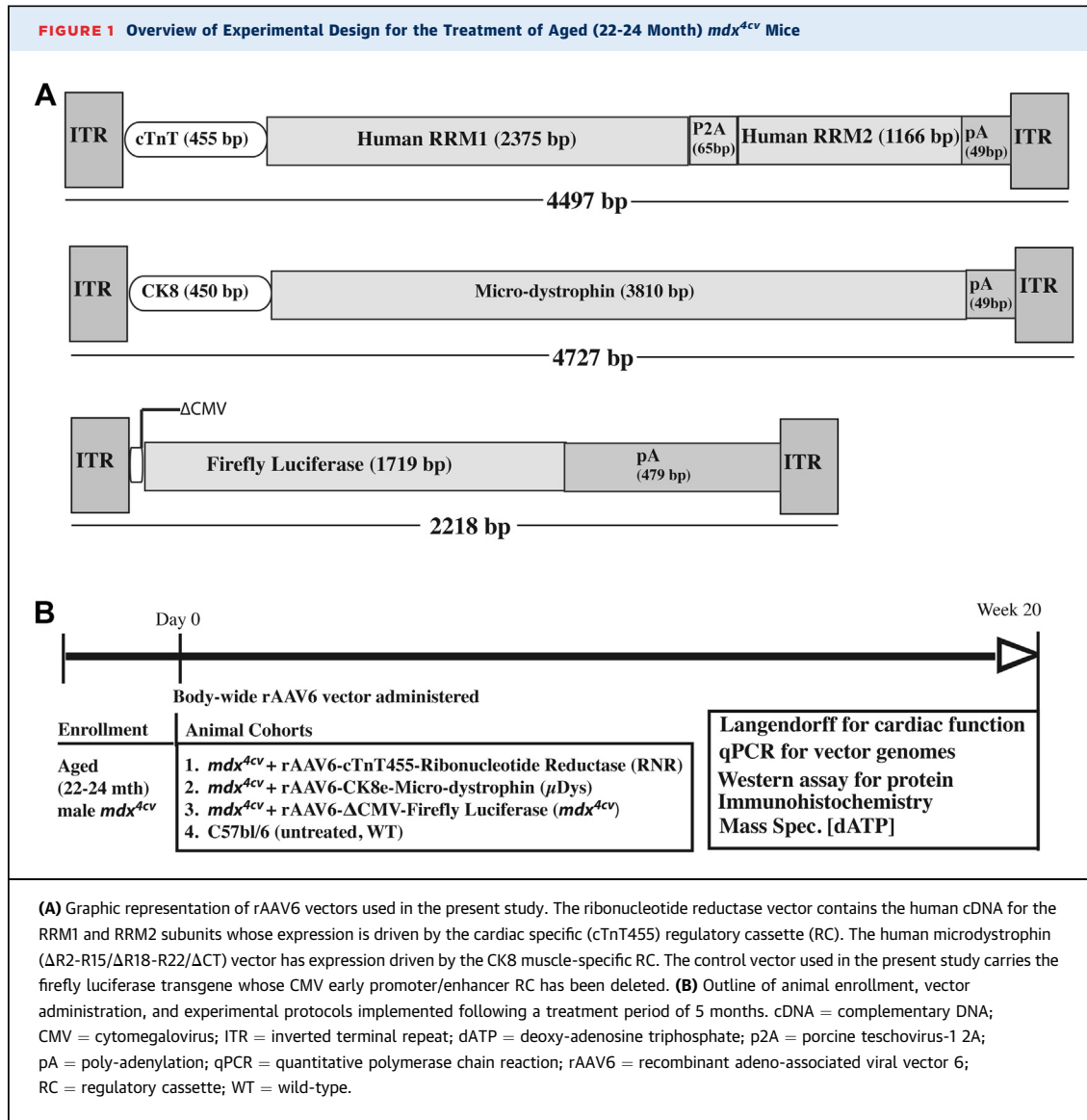
RESULTS

IMPROVEMENTS IN BASELINE CARDIAC FUNCTION IN VECTOR-TREATED MDX^{4cv} HEARTS.

As depicted in **Figure 1**, 22- to 24-month-old *mdx*^{4cv} mice were administered 1 of 3 treatments: rAAV6-cTnT455-RNR (referred to as *mdx*^{4cv}+RNR); rAAV6-CK8- μ Dys (referred to as *mdx*^{4cv}+ μ Dys), or rAAV6- Δ CMV-Firefly Luciferase control vector (referred to as *mdx*^{4cv}) at a dose of 2×10^{14} vg/kg. By the end of the 20-week treatment period, both *mdx*^{4cv}+RNR and *mdx*^{4cv}+ μ Dys mice showed improvements in survival rates compared to *mdx*^{4cv} mice, although this did not reach statistical significance (**Supplemental Figure 1**). At the end of 5 months, an extensive evaluation of ex vivo cardiac function using the Langendorff isolated heart preparation was performed. The isolated heart technique allows for the direct assessment of inherent myocardial function without the confounding effects of neuro-humoral or other systemic variables. An additional cohort of age-matched, untreated C57BL6 mice (WT) was used as comparison control. At baseline, RPP was significantly decreased in *mdx*^{4cv} hearts due to an approximate 20% decrease in LVDevP (**Supplemental Figures 1A and 1B**). RNR-treated *mdx*^{4cv} mice exhibited a restoration of RPP ($p = 0.056$) primarily due to a normalization of LVDevP (**Supplemental Figures 2A and 2B**). Although μ Dys-treated *mdx*^{4cv} hearts appeared to normalize LVDevP, this did not lead to a significant improvement in RPP (**Supplemental Figures 2A and 2B**). Both +dP/dt and -dP/dt, an index of ventricular contractility and relaxation, respectively, were decreased 30% in *mdx*^{4cv} hearts ($p = 0.061$). The +dP/dt was similar to control in both RNR-treated *mdx*^{4cv} and μ Dys-treated *mdx*^{4cv} hearts. However, only RNR-treated *mdx*^{4cv} hearts showed -dP/dt values similar to control levels (**Supplemental Figures 2C and 2D**).

POSITIVE CHANGES IN FRANK-STARLING MECHANICS IN VECTOR-TREATED MDX^{4cv} HEARTS.

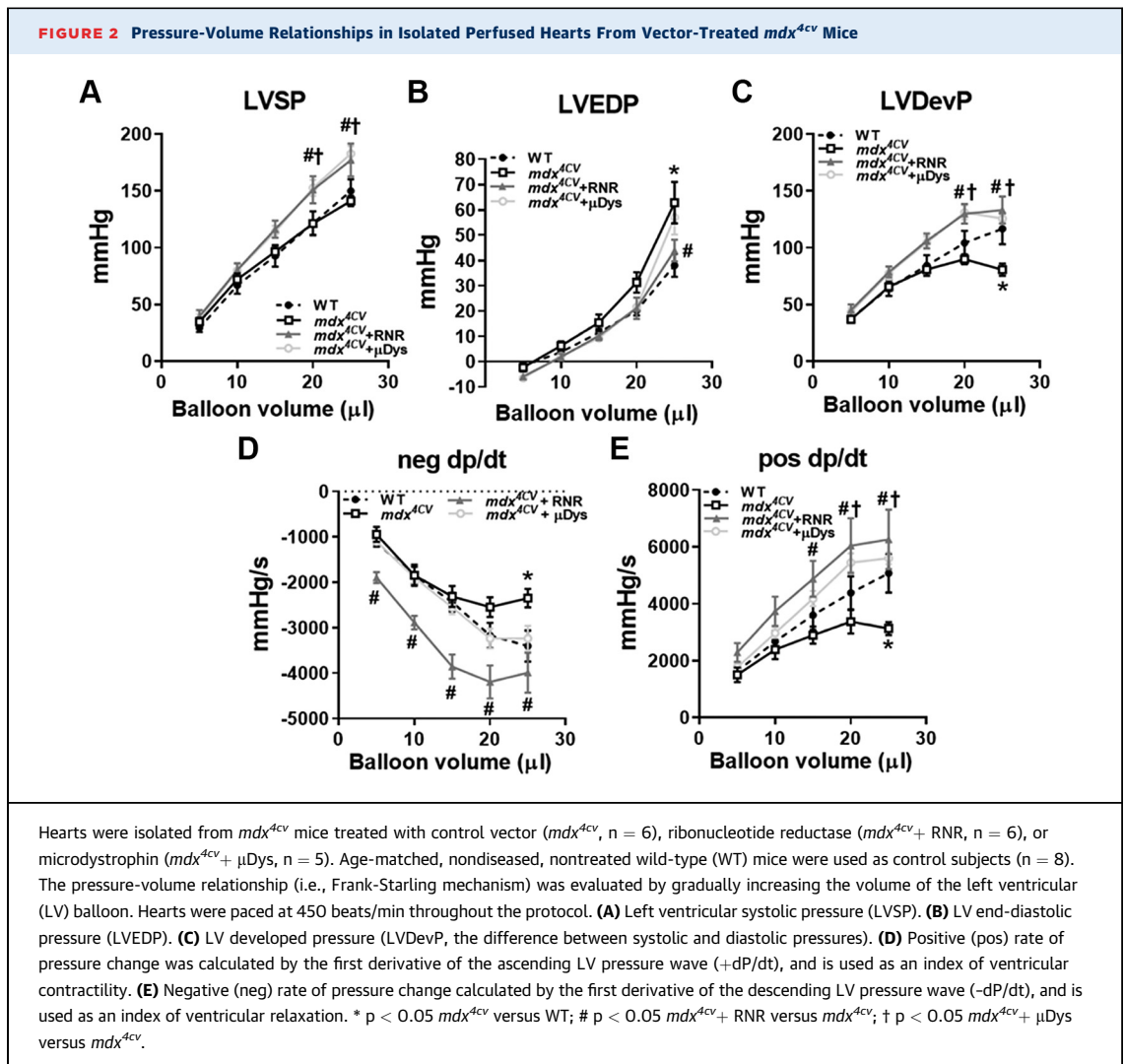
To evaluate further systolic and diastolic function in vector-treated *mdx*^{4cv} hearts, we examined the pressure-volume relationship (i.e., Frank-Starling mechanism) in the isolated perfused heart preparation. The LVSP response to increased preload was significantly improved in both in *mdx*^{4cv}+RNR and *mdx*^{4cv}+ μ Dys hearts compared to *mdx*^{4cv} (**Figure 2A**). However, only RNR treatment improved the diastolic response in *mdx*^{4cv} hearts, to levels similar to WT (**Figure 2B**). Both contractility and relaxation (i.e., +dP/dt and



-dP/dt, respectively) were impaired in *mdx*^{4cv} compared to age-matched control subjects (Figures 2D and 2E). Both *mdx*^{4cv}+ RNR and *mdx*^{4cv}+ μ Dys hearts had significantly elevated +dP/dt values above *mdx*^{4cv} (Figure 2D). Interestingly, treatment of *mdx*^{4cv} hearts with RNR also significantly improved -dP/dt values (Figure 2E). All told, these data suggest that both RNR and μ Dys treatment can improve systolic function in *mdx*^{4cv} hearts. However, only the RNR treatment corrected diastolic dysfunction in *mdx*^{4cv} hearts.

AUGMENTED RESPONSE TO INCREASED CARDIAC WORKLOAD IN TREATED MDX^{4CV} HEARTS. We previously reported that RNR overexpression in transgenic or vector-treated mouse hearts elevated

baseline function but did not impair the response to a short-term physiologic increase in cardiac work (47,48). To verify that the improved systolic and diastolic function in RNR-treated *mdx*^{4cv} hearts at baseline was not associated with an inability to respond to an increased energetic demand, we stressed hearts with a combination of high calcium and elevated heart rates, via pacing stimulation. As shown in Figures 3A and 3B, *mdx*^{4cv} hearts had a blunted response to the increased workload as both LVDevP and RPP were ~25% to 30% lower than WT hearts. In addition, both +dP/dt and -dP/dt were impaired in *mdx*^{4cv} relative to WT hearts (Figures 3C and 3D). Systolic parameters in *mdx*^{4cv}+ μ Dys hearts were effectively improved and similar to age-matched WT hearts for the entire duration of the workload challenge

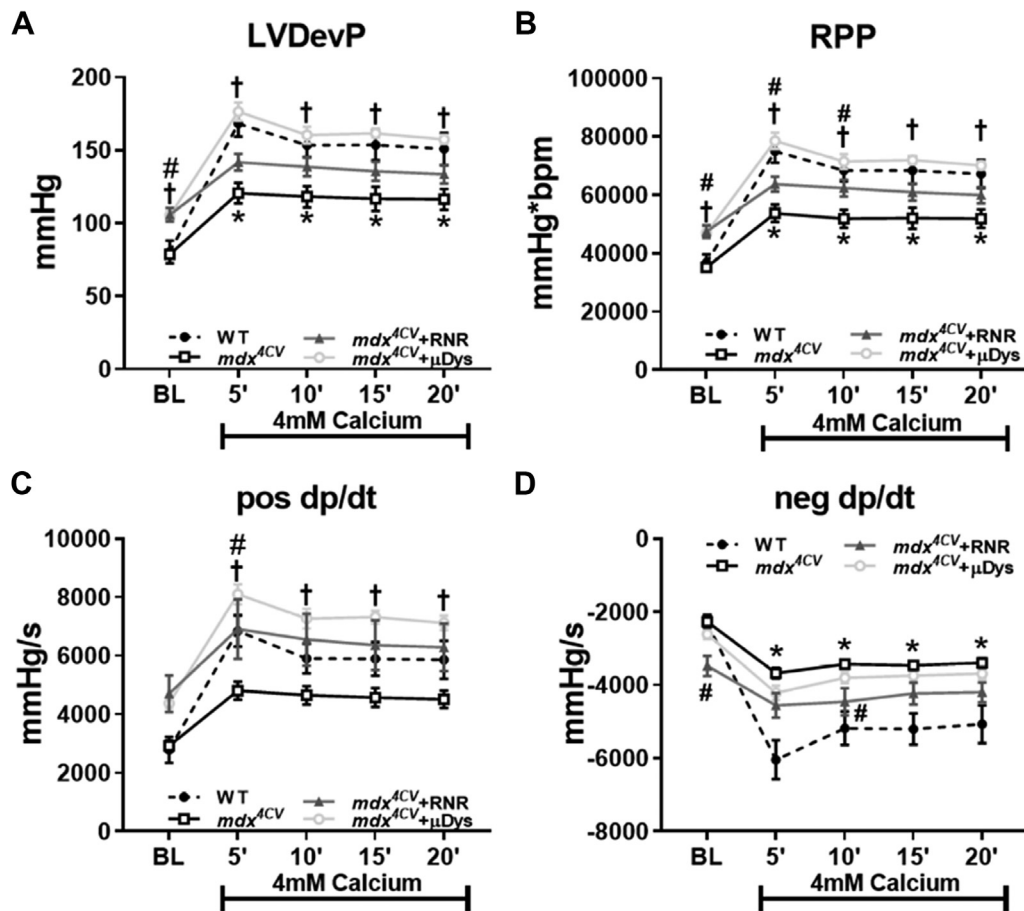


(Figures 3A to 3C). Measures of systolic function significantly increased in *mdx*^{4cv} + RNR hearts during the initial half of the high workload protocol and remained ~15% higher than *mdx*^{4cv} (Figures 3A to 3C). Interestingly, -dP/dt values tended to be elevated only in *mdx*^{4cv} + RNR hearts during the physiologic challenge (Figure 3D). These data show that both RNR and μ Dys treatments improve systolic function in *mdx*^{4cv} hearts without compromising cardiac reserve. Combined with the baseline and pressure-volume relationship assessments, our data show that, in addition to the systolic enhancements, RNR has an added benefit of improving diastolic function.

RNR AND μ Dys TRANSDUCTION, EXPRESSION, AND CARDIOMYOCYTE LOCALIZATION. To evaluate the localization of RNR and μ Dys protein within the hearts of mice, we performed immunofluorescence imaging. As shown in Figure 4, the RNR subunit (Rrm1) was robustly expressed in ventricles of RNR-treated mice.

The expression of μ Dys appeared to be saturated relative to full-length dystrophin levels, with both being properly localized to the sarcolemma of cardiomyocytes. We also evaluated general muscle histopathology and potential differences in myocardial fibrosis by Masson trichrome staining, and observed no discernable difference between treated or untreated *mdx*^{4cv} mice (Figure 5). In addition, neither RNR nor μ Dys treatment significantly altered body weight, heart weight, or the heart weight-to-body weight ratio (Supplemental Figure 3). Western blotting was performed to determine the extent of rAAV vector 6-mediated RNR and μ Dys protein expression profiles in ventricular tissue (Figure 6). We observed μ Dys protein expression in ventricular tissue that approached levels similar to WT mice, whereas both human RNR subunits were found to be elevated to comparable levels within ventricular tissue (Figure 6A). To evaluate the relative proportions of

FIGURE 3 The Response of Vector-Treated *mdx^{4cv}* Mice to High Workload Challenge in Langendorff Isolated Heart Preparations

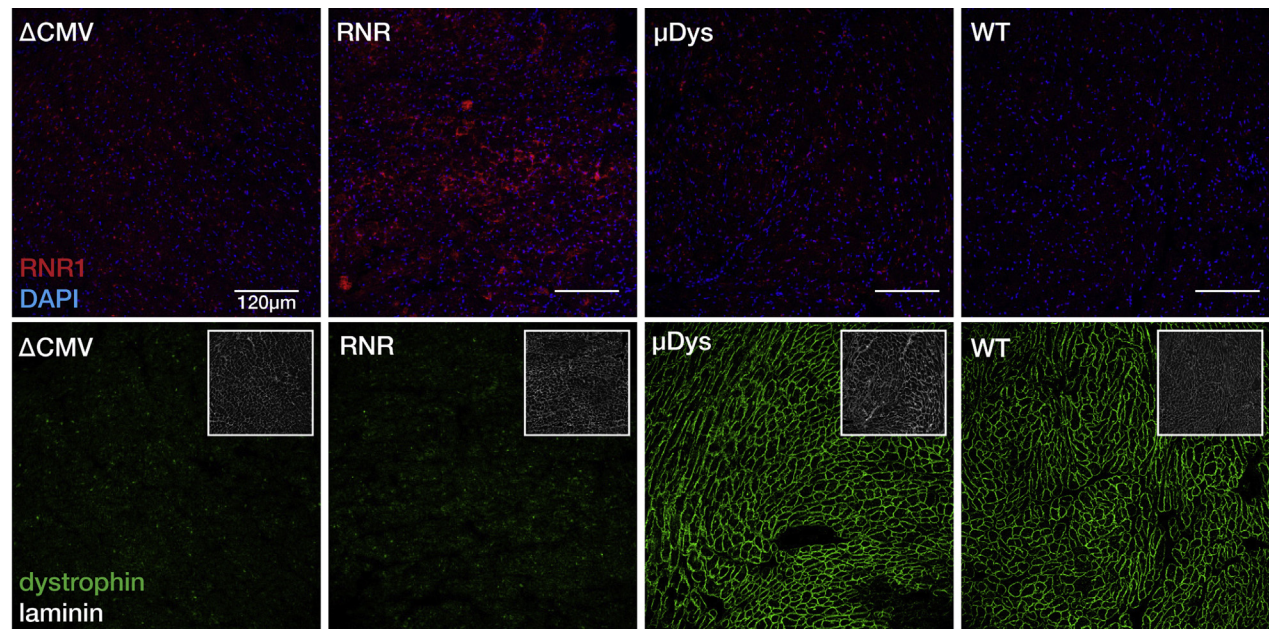


Hearts were isolated from *mdx^{4cv}* mice treated with control vector (*mdx^{4cv}*, n = 6), ribonucleotide reductase (*mdx^{4cv}*+ RNR, n = 6), or microdystrophin (*mdx^{4cv}*+ μ Dys, n = 5). Age-matched, nondiseased, nontreated wild-type (WT) mice were used as control subjects (n = 4). All hearts were perfused with a glucose-pyruvate buffer containing high calcium (4.0 mmol/l) to simulate a high workload challenge for 20 min. Hearts were paced at 450 beats per minute throughout the protocol. **(A)** LVDevP (the difference between systolic and diastolic pressures). **(B)** Rate pressure product (RPP, the product of LVDevP and HR). **(C)** Positive rate of pressure change calculated by the first derivative of the ascending LV pressure wave (+dP/dt), is used as an index of ventricular contractility. **(D)** Negative rate of pressure change calculated by the first derivative of the descending LV pressure wave (-dP/dt), is used as an index of ventricular relaxation. * p < 0.05 *mdx^{4cv}* versus WT; # p < 0.05 *mdx^{4cv}*+ RNR versus *mdx^{4cv}*; † p < 0.05 *mdx^{4cv}*+ μ Dys versus *mdx^{4cv}*. Abbreviations as in **Figures 1 and 2**.

dATP concentrations within ventricular tissue, we performed HPLC-MS/MS analysis on ground ventricular tissue from *mdx^{4cv}* and *mdx^{4cv}*+ RNR mice. The concentration of dATP within the ventricular tissue obtained from *mdx^{4cv}* mice treated with RNR (0.57 ± 0.22 pmol dATP/mg) was approximately 10-fold higher relative to *mdx^{4cv}* control subjects (0.05 ± 0.02 pmol dATP/mg) (**Figure 6B**). For adult WT, we previously reported an average dATP value of 0.02 pmol/mg tissue with a SD of 0.01 (50). Additionally, cardiac vector genome data was comparable relative to the vector dose administered (**Figure 6C**).

DISCUSSION

In the present study, we used a novel gene therapy approach that targets myosin in the contractile filaments of cardiomyocytes via overexpression of the RNR enzyme to rescue cardiomyopathy in a DMD mouse model. RNR overexpression results in elevated dATP, which can be used by cardiac myosin (in place of ATP), and increases cross-bridge binding and cycling, resulting in stronger, faster contraction and faster relaxation (38-45,52). We developed an rAAV vector that over-expresses RNR selectively in heart

FIGURE 4 Cardiac Transduction Following Intravenous Delivery of Ribonucleotide Reductase or Microdystrophin

At 5 months after vector administration, cryosections were prepared and immunostained with antisera against dystrophin or ribonucleotide reductase. A considerable level of protein is detected for each ribonucleotide reductase subunit-1 (human specific) as indicated by immunofluorescent staining (red) localized primarily within the cytoplasm of cardiomyocytes with occasional perinuclear accumulation (upper panel). On the lower panel, the robust level of expression for dystrophin in WT and in aged *mdx*^{Δcv} mice treated with AAV6-CK8-μDys (laminin staining, inset image). Abbreviations as in Figures 1 and 2.

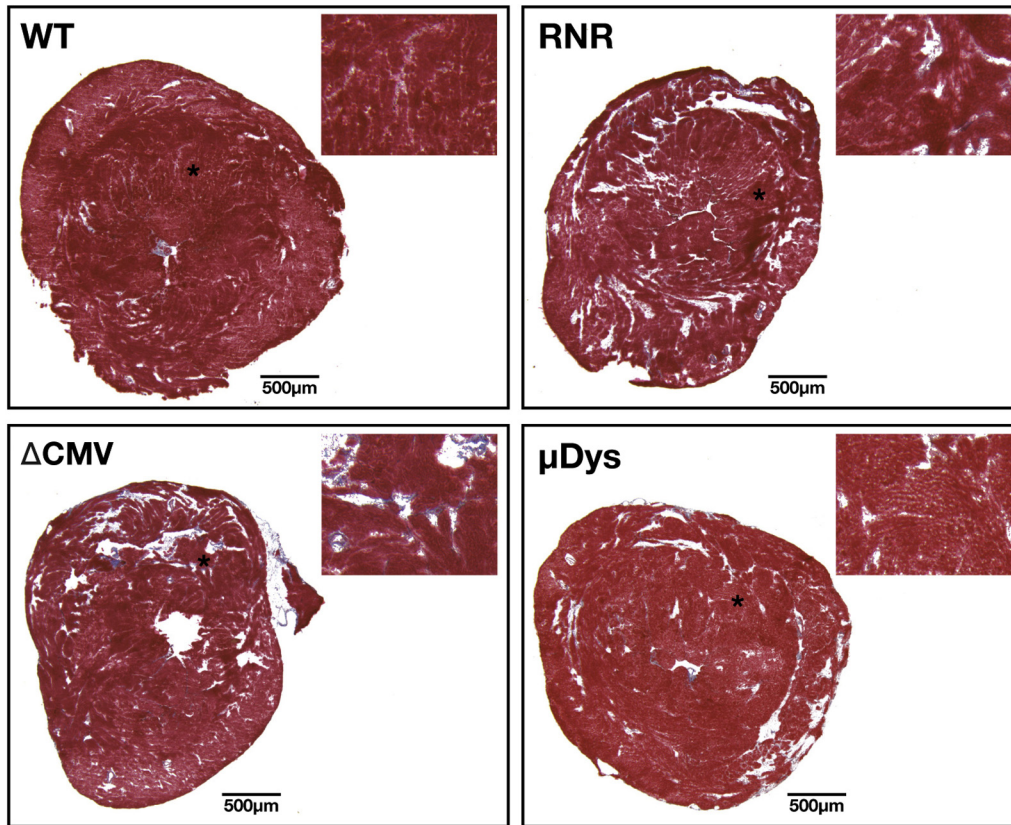
muscle via inclusion of a modified cardiac-specific enhancer/promoter derived from the human cTnT gene, which facilitates increases in myocyte contraction and cardiac performance in normal rodent hearts as well as in infarcted rodents and pig hearts (48,53). Importantly, we previously showed that dATP-producing cells deliver it to surrounding myocardium by diffusion through gap junctions (54), such that only a minority of cardiomyocytes needs to be transduced to have global benefits within the heart. We now show that using this vector technology leads to a clear benefit of improving cardiac function in an advanced-age model of DMD cardiomyopathy.

Early manifestations of impaired cardiac dysfunction in *mdx* mice are generally not reported. Khairallah et al.(55) observed a decline in LV function in isolated perfused hearts that coincided with decreased fatty acid oxidation and increased glucose oxidation. However, perfused heart function in *mdx* mice was maintained at 8 months, despite significant reductions in phosphocreatine levels and free energy availability from ATP hydrolysis (56). The authors surmised that young adult *mdx* hearts, akin to DMD patient hearts, experience right ventricular dilation, LV diastolic deficits, and abnormal energy

metabolism. More recently, a declination in cardiac function was not observed until 12 months of age (57) and abnormal in vivo pressure-volume dynamics were observed in 22-month-old *mdx* mice (58). Treatment of young male *mdx* mice with rAAV6 vector delivering cytomegalovirus (CMV) promoter/enhancer driven microdystrophin did not correct the impairments in +dP/dt, -dP/dt, or LV systolic pressure when assessed at 5 months of age via hemodynamic analysis (35). However, an improvement was noted for the preload recruited stroke work in *mdx* mice treated with μDys compared to untreated *mdx* or WT control subjects (35).

In our current study, 27-month to 29-month-old mice were subjected to ex vivo assessment of cardiac function using the Langendorff isolated heart preparation, which is a century-old methodology with several advantages and limitations (59). The perfusate used is similar to, but not the same as blood, and situations of physiologic challenge (e.g., Frank-Starling and high calcium) may exaggerate the in vivo situation. However, the procedure remains a simple and reproducible experiment that allows for interrogation of cardiac physiology in the absence of confounding systemic variables and serves as a viable

FIGURE 5 Heart Histologic Staining of *mdx*^{4cv} Mice Suggests No Morphologic Alterations From RNR Therapy

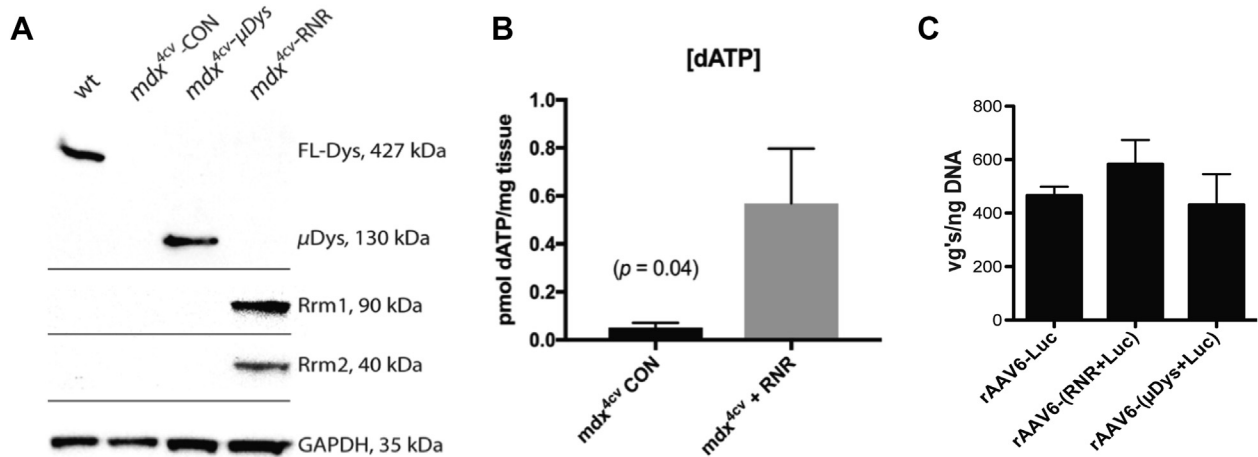


Representative full-view photomicrographs of Masson trichrome staining of the hearts from *mdx*^{4cv} mice displaying control vector (Δ CMV), and rAAV6-treated with either RNR or μ Dys from *mdx*^{4cv} mice. Similarly, a 20 \times enlarged view of the corresponding images (*) is shown. Abbreviations as in [Figures 1 and 2](#).

tool to perform cardiac phenotyping in preclinical studies (60). Under baseline conditions and at spontaneous heart rates, we observed a significant reduction in RPP in *mdx*^{4cv} hearts. Decreased systolic and diastolic performance in *mdx*^{4cv} hearts also existed while examining the length-tension relationship (i.e., Frank-Starling mechanism). Treatment of *mdx*^{4cv} mice with either the RNR or the μ Dys vector restored systolic pressure development without affecting spontaneous HRs at baseline. Both of the treatments restored the disrupted Frank-Starling response, particularly for systolic function. The RNR treatment also had beneficial effects on the diastolic properties of the *mdx*^{4cv} myocardium. This strongly supports our previous studies where we observed a tendency for overexpression of RNR to improve myocardial diastolic response in young, healthy, transgenic mice (47), mice treated with AAV (48), and in a porcine HF model (53).

In addition to the evaluation of basal cardiac performance, we tested cardiac reserve with a combination of high calcium plus elevated HRs and confirmed a significantly blunted response in 27-month to 29-month-old *mdx*^{4cv} hearts. Consistent with a previous report in young *mdx* mice (35), expressing μ Dys in aged *mdx*^{4cv} hearts significantly improved systolic performance during increased physiologic demand to a level similar to age-matched healthy control subjects. We previously reported that transgenic or vector-directed overexpression of RNR did not impair cardiac reserve during increased physiologic demand in young healthy hearts (47,48). Herein, we report that RNR over-expression in *mdx*^{4cv} hearts normalizes both the systolic and diastolic response to an increased cardiac challenge.

Approximately two-thirds of DMD mutations are deletions that span 1 or more exons, often leading to large deletions clustering around 2 mutational

FIGURE 6 Protein Expression Levels for μ Dys, RNR, and Resultant Vector Genomes Due to rAAV6-Mediated Gene Transfer

(A) RNR and μ Dys protein expression detection as revealed by immunoblotting of cardiac whole tissue lysates using either RRM1, RRM2, or antidystrophin antibody. **(B)** HPLC-MS/MS intracellular [dNTP] quantification from methanol extracted cardiac tissue. **(C)** qPCR analysis of vector genomes from cardiac tissue revealed similar vector genomes being represented for all treated cohorts. dNTP = deoxynucleotide triphosphate; HPLC-MS/MS = high-performance liquid chromatography-tandem mass spectrometry; qPCR = quantitative polymerase chain reaction; other abbreviations as in [Figures 1 and 2](#).

hotspots; the most common spanning from exons 45-55 resulting in removal of a central portion of the rod domain inclusive of disrupting the neuronal nitric oxide synthase (nNOS) localization domain. The second most common hotspot spans from exons 3-19, and removes the majority of the amino-terminal actin-binding domain 1 which is essential for dystrophin function. When such deletions interrupt the reading frame, the resultant mutated protein usually expresses at extremely low levels and associates with the loss of ambulation at or before 12 years of age. Even when such deletions produce an in-frame partially functional truncated protein, such as occurs in BMD, dramatic phenotype diversity can occur. For example, in a previous study, BMD subjects whose out-of-phase deletions, toward the alignment of adjoining spectrin-like repeats, developed dilated cardiomyopathy at nearly a decade earlier than in patients with in-phase deletions (61). In contrast to large deletion mutations, there are reported cases where individual missense mutations lead to X-linked dilated cardiomyopathy (62-64). In one case, a novel missense mutation within exon 9 at nucleotide 1043 resulted in a T279A amino acid change in a highly conserved position of mutation. This mutation resulted in a substitution of a beta-sheet for alpha-helical structure, destabilizing the protein, and leading to the cardiac specific phenotype described by the authors (63).

DMD-related cardiomyopathy usually occurs during middle to late adolescence, but the clinical presentation is deceptive, as patients are wheelchair-bound and are not required to perform increased cardiac workload. The diversity of cardiac phenotype in DMD suggests many levels of pathogenic mechanisms. The pathologic heterogeneity of the DMD ventricular myocardium is a consequential result of myocardial atrophy (65,66), compensatory mechanisms leading to cardiac remodeling with ensuing ventricular dilation and fibrosis (67,68). Absence of clear genotype-phenotype correlation in DMD probably results from at least 4 secondary cellular processes including aberrant intracellular Ca^{2+} homeostasis, decreased nitric oxide-cyclic guanosine monophosphate pathways, mitochondrial dysfunction, and increased reactive oxygen species, which individually or collectively influence the clinical phenotype (69). As an indication of the progressive nature of DMD cardiomyopathy, the estimated overall incidence of latent DCM is 25% by 6 years of age and 59% by 10 years of age in DMD patients (70). As such, further evidence suggests latency in cardiac dysfunction at basal levels that becomes more pronounced with an induction of increased physiological demand. Consistent with these observations, an impaired response to beta-adrenergic stimulation by either dobutamine or isoproterenol can be detected in *mdx* mice at 3 to 4 months of age (35,71). Exercise can

potentially be a double-edged sword for DMD, where the enthusiasm for potential skeletal muscle benefits can be dampened by the insidious cardiotoxicity from training (72–74). With gene replacement therapy via rAAV-mediated μ Dys in current ongoing clinical trials, it will be of interest to assess cardiac function to determine whether additional therapeutic support in the form of increased contractility will be beneficial.

Relative expression assays by immunofluorescence and Western blotting indicate robust expression levels for the RNR subunits (RRM1 and RRM2) and μ Dys in the vast majority of cardiomyocytes. However, intracellular variability in RNR protein detection (via immunostaining) was observed for both RRM1 and RRM2, indicating that not all cardiomyocytes were effectively transduced. Nevertheless, we previously have shown that gap junction transport of dATP from transduced cardiomyocytes to adjacent cardiomyocytes occurs (54), which likely accounted for the consistently elevated LV function of mice treated with the rAAV vector that over-expresses RNR. This is in contrast to the anchored sarcolemma localization of μ Dys, which would occur only in transduced muscle cells. Additionally, because muscle-specific regulatory cassettes were used for expression of therapeutic proteins, we can surmise that <1% of protein expression would be generated from non-muscle cell types present in the heart, suggesting that the functional benefit was truly caused by cardiomyocyte transduction. As previously stated, the cTnT regulatory cassette drives RNR expression only in heart muscle, whereas the CK8 regulatory cassette drives μ Dys expression no selectively in both cardiac and skeletal muscle cells, but at only very low background levels in other tissues. This raises the possibility that the functional benefit of expressing μ Dys in skeletal muscles might increase energetic demands on the heart, thereby partially masking some of the μ Dys-derived cardiac functional benefits (37). Because RNR delivery to DMD mice of advanced age increased cardiac function in the absence of RNR expression in skeletal muscle, and because over-expression of endogenous RNR should

be nonimmunogenic, supplemental RNR therapy in conjunction with μ Dys therapy might be beneficial for DMD patients. Future studies are aimed at determining the extent of functional restoration by combining both RNR- and μ Dys-based therapies.

ACKNOWLEDGMENTS The authors thank James Allen and Christine Halbert (Wellstone Muscular Dystrophy Specialized Research Center, University of Washington, Seattle, Washington) for assistance with vector production, purification, and quality assessment.

ADDRESS FOR CORRESPONDENCE: Dr. Guy L. Odom, Department of Neurology, University of Washington, 850 Republican Street, S248, Box 358055, Seattle, Washington 98109. E-mail: godom@uw.edu. OR Dr. Michael Regnier, Department of Bioengineering, University of Washington, 850 Republican Street, S180, Seattle, Washington 98109. E-mail: mregnier@uw.edu.

PERSPECTIVES

COMPETENCY IN MEDICAL KNOWLEDGE: RNR over-expression represents an emerging therapy for improving cardiac dysfunction via cardiac myosin activation in a variety of clinical situations. Currently, there are 3 ongoing clinical trials using rAAV-mediated variants of μ Dys that have shown broad promise in terms of safety, and in biomarker indicators suggesting pathologic improvements. If cardiac dysfunction is detected in the patients from these clinical studies, our studies in aged, *mdx* mice suggest that combinatorial RNR therapy may be beneficial.

TRANSLATIONAL OUTLOOK: Our novel strategy of vector-mediated, cardiac-specific over-expression of RNR shows promising potential for rescuing both systolic and diastolic function in aged, DMD mice even in the absence of addressing the underlying dystrophin deficiency. Future studies investigating the combined effects of μ Dys and RNR may disclose an improved therapeutic strategy to provide structural and functional improvement of DMD patient hearts.

REFERENCES

1. Emery AE, Muntoni F. *Duchenne Muscular Dystrophy*. 3rd ed. Oxford, United Kingdom: Oxford University Press, 2003:270.
2. Ervasti JM. Structure and function of the dystrophin-glycoprotein complex. In: Winder SJ, editor. *Molecular Mechanisms of Muscular Dystrophies*. Georgetown, Texas: Landes Biosciences, 2006:1-13.
3. Cox GA, Phelps SF, Chapman VM, Chamberlain JS. New *mdx* mutation disrupts expression of muscle and nonmuscle isoforms of dystrophin. *Nature Genet* 1993;4:87-93.
4. Brooks SV, Faulkner JA. Contractile properties of skeletal muscles from young, adult and aged mice. *J Physiol (London)* 1988;404:71-82.
5. Campbell KP. Three muscular dystrophies: loss of cytoskeleton-extracellular matrix linkage. *Cell* 1995;80:675-9.
6. Petrof BJ, Shrager JB, Stedman HH, Kelly AM, Sweeney HL. Dystrophin protects the sarcolemma from stresses developed during muscle contraction. *Proc Natl Acad Sci U S A* 1993;90:3710-4.

7. Ramaswamy KS, Palmer ML, van der Meulen JH, et al. Lateral transmission of force is impaired in skeletal muscles of dystrophic mice and very old rats. *J Physiol* 2011;589 Pt 5:1195-208.
8. Chao DS, Gorospe JR, Brenman JE, et al. Selective loss of sarcolemmal nitric oxide synthase in Becker muscular dystrophy. *J Exp Med* 1996;184:609-18.
9. Froehner SC. Just say NO to muscle degeneration? *Trends Mol Med* 2002;8:51-3.
10. Grady RM, Grange RW, Lau KS, et al. Role for alpha-dystrobrevin in the pathogenesis of dystrophin-dependent muscular dystrophies. *Nat Cell Biol* 1999;1:215-20.
11. Lapidus KA, Kakkar R, McNally EM. The dystrophin glycoprotein complex: signaling strength and integrity for the sarcolemma. *Circ Res* 2004;94:1023-31.
12. Ervasti JM, Campbell KP. A role for the dystrophin-glycoprotein complex as a transmembrane linker between laminin and actin. *J Cell Biol* 1993;122:809-23.
13. Ibraghimov-Beskrovnyaya O, Ervasti JM, Leveille CJ, et al. Primary structure of dystrophin-associated glycoproteins linking dystrophin to the extracellular matrix. *Nature* 1992;355:696-702.
14. Yoshida M, Ozawa E. Glycoprotein complex anchoring dystrophin to sarcolemma. *J Biochem (Tokyo)* 1990;108:748-52.
15. England SB, Nicholson LV, Johnson MA, et al. Very mild muscular dystrophy associated with the deletion of 46% of dystrophin. *Nature* 1990;343:180-2.
16. Valentine BA, Winand NJ, Pradhan D, et al. Canine X-linked muscular dystrophy as an animal model of Duchenne muscular dystrophy: a review. *Am J Med Genet* 1992;42:352-6.
17. Im WB, Phelps SF, Copen EH, et al. Differential expression of dystrophin isoforms in strains of mdx mice with different mutations. *Hum Mol Genet* 1996;5:1149-53.
18. Phelps SF, Hauser MA, Cole NM, et al. Expression of full-length and truncated dystrophin mini-genes in transgenic *mdx* mice. *Hum Mol Genet* 1995;4:1251-8.
19. Crawford GE, Faulkner JA, Crosbie RH, et al. Assembly of the dystrophin-associated protein complex does not require the dystrophin COOH-terminal domain. *J Cell Biol* 2000;150:1399-410.
20. Harper SQ, Hauser MA, DelloRusso C, et al. Modular flexibility of dystrophin: implications for gene therapy of Duchenne muscular dystrophy. *Nat Med* 2002;8:253-61.
21. Wang B, Li J, Xiao X. Adeno-associated virus vector carrying human minidystrophin genes effectively ameliorates muscular dystrophy in mdx mouse model. *Proc Natl Acad Sci U S A* 2000;97:13714-9.
22. Sakamoto M, Yuasa K, Yoshimura M, et al. Micro-dystrophin cDNA ameliorates dystrophic phenotypes when introduced into mdx mice as a transgene. *Biochem Biophys Res Commun* 2002;293:1265-72.
23. Chamberlain JS. Gene therapy of muscular dystrophy. *Hum Mol Genet* 2002;11:2355-62.
24. Hakim CH, Wasala NB, Pan X, et al. A five-repeat micro-dystrophin gene ameliorated dystrophic phenotype in the severe DBA/2J-mdx model of Duchenne muscular dystrophy. *Mol Ther Methods Clin Dev* 2017;6:216-30.
25. Cox GA, Cole NM, Matsumura K, et al. Overexpression of dystrophin in transgenic mdx mice eliminates dystrophic symptoms without toxicity [see comments]. *Nature* 1993;364:725-9.
26. Stedman HH, Sweeney HL, Shrager JB, et al. The mdx mouse diaphragm reproduces the degenerative changes of Duchenne muscular dystrophy. *Nature* 1991;352:536-9.
27. Brooks SV, Faulkner JA. Skeletal muscle weakness in old age: underlying mechanisms. *Med Sci Sports Exerc* 1994;26:432-9.
28. DelloRusso C, Crawford R, Chamberlain J, Brooks S. Tibialis anterior muscles of *mdx* mice are highly susceptible to contraction-induced injury. *J Muscle Res Cell Motility* 2001;22:467-75.
29. Lynch GS, Hinkle RT, Chamberlain JS, Brooks SV, Faulkner JA. Force and power output of fast and slow skeletal muscles from mdx mice 6-28 months old. *J Physiol* 2001;535 Pt 2:591-600.
30. Bostick B, Shin JH, Yue Y, et al. AAV micro-dystrophin gene therapy alleviates stress-induced cardiac death but not myocardial fibrosis in >21-m-old mdx mice, an end-stage model of Duchenne muscular dystrophy cardiomyopathy. *J Mol Cell Cardiol* 2012;53:217-22.
31. Gregorevic P, Blankinship MJ, Allen JM, Chamberlain JS. Systemic microdystrophin gene delivery improves skeletal muscle structure and function in old dystrophic mdx mice. *Mol Ther* 2008;16:657-64.
32. Quinlan JG, Hahn HS, Wong BL, et al. Evolution of the mdx mouse cardiomyopathy: physiological and morphological findings. *Neuromuscul Disord* 2004;14:491-6.
33. Gregorevic P, Allen JM, Minami E, et al. rAAV6-microdystrophin preserves muscle function and extends lifespan in severely dystrophic mice. *Nat Med* 2006;12:787-9.
34. Shin JH, Nishihara-Kasahara Y, Hayashita-Kinoh H, et al. Improvement of cardiac fibrosis in dystrophic mice by rAAV9-mediated micro-dystrophin transduction. *Gene Ther* 2011;18:910-9.
35. Townsend D, Blankinship MJ, Allen JM, et al. Systemic administration of micro-dystrophin restores cardiac geometry and prevents dobutamine-induced cardiac pump failure. *Mol Ther* 2007;15:1086-92.
36. Bostick B, Shin JH, Yue Y, Duan D. AAV-microdystrophin therapy improves cardiac performance in aged female mdx mice. *Mol Ther* 2011;19:1826-32.
37. Townsend D, Yasuda S, Chamberlain J, Metzger JM. Cardiac consequences to skeletal muscle-centric therapeutics for Duchenne muscular dystrophy. *Trends Cardiovasc Med* 2009;19:50-5.
38. Adhikari BB, Regnier M, Rivera AJ, Kreutziger KL, Martyn DA. Cardiac length dependence of force and force development kinetics with altered cross-bridge cycling. *Biophysical J* 2004;87:1784-94.
39. Clemmens EW, Entezari M, Martyn DA, Regnier M. Different effects of cardiac versus skeletal muscle regulatory proteins on in vitro measures of actin filament speed and force. *J Physiol* 2005;566 Pt 3:737-46.
40. Korte FS, Dai J, Buckley K, et al. Upregulation of cardiomyocyte ribonucleotide reductase increases intracellular 2 deoxy-ATP, contractility, and relaxation. *J Mol Cell Cardiol* 2011;51:894-901.
41. Kreutziger KL, Piroddi N, McMichael JT, Poggesi C, Tesi C, Regnier M. Cooperative activation and tension kinetics in cardiac muscle are strongly modulated by calcium binding kinetics of troponin C. *J Mol Cell Cardiol* 2011;50:165-74.
42. Moussavi-Harami F, Razumova MV, Racca AW, et al. 2-deoxy adenosine triphosphate improves contraction in human end-stage heart failure. *J Mol Cell Cardiol* 2015;79:256-63.
43. Regnier M, Lee DM, Homsher E. ATP analogs and muscle contraction: mechanics and kinetics of nucleoside triphosphate binding and hydrolysis. *Biophys J* 1998;74:3044-58.
44. Regnier M, Martin H, Barsotti RJ, et al. Cross-bridge versus thin filament contributions to the level and rate of force development in cardiac muscle. *Biophys J* 2004;87:1815-24.
45. Regnier M, Rivera AJ, Chen Y, Chase PB. 2-deoxy-ATP enhances contractility of rat cardiac muscle. *Circ Res* 2000;86:1211-7.
46. Cheng Y, Hogarth KA, O'Sullivan ML, Regnier M, Pyle WG. 2-deoxyadenosine triphosphate restores the contractile function of cardiac myofibril from adult dogs with naturally occurring dilated cardiomyopathy. *Am J Physiol Heart Circ Physiol* 2016;310:H80-91.
47. Nowakowski SG, Kolwicz SC, Korte FS, et al. Transgenic overexpression of ribonucleotide reductase improves cardiac performance. *Proc Natl Acad Sci U S A* 2013;110:6187-92.
48. Kolwicz SC Jr., Odom GL, Nowakowski SG, et al. AAV6-mediated cardiac-specific overexpression of ribonucleotide reductase enhances myocardial contractility. *Mol Ther* 2016;24:240-50.
49. Halbert CL, Allen JM, Chamberlain JS. AAV6 vector production and purification for muscle gene therapy. *Methods Mol Biol* 2018;1687:257-66.
50. Olafsson S, Whittington D, Murray J, Regnier M, Moussavi-Harami F. Fast and sensitive HPLC-MS/MS method for direct quantification of intracellular deoxyribonucleoside triphosphates from tissue and cells. *J Chromatogr B Analyt Technol Biomed Life Sci* 2017;1068-1069:90-7.
51. Kolwicz SC Jr., Tian R. Assessment of cardiac function and energetics in isolated mouse hearts using ³¹P NMR spectroscopy. *J Vis Exp* 2010;42:e2069.
52. Kreutziger KL, Piroddi N, Belus A, Poggesi C, Regnier M. Ca²⁺-binding kinetics of troponin C influence force generation kinetics in cardiac muscle. *Biophysical J* 2007;92:477a.
53. Kadota S, Carey J, Reinecke H, et al. Ribonucleotide reductase-mediated increase in dATP

improves cardiac performance via myosin activation in a large animal model of heart failure. *Eur J Heart Fail* 2015;17:772-81.

54. Lundy SD, Murphy SA, Dupras SK, et al. Cell-based delivery of dATP via gap junctions enhances cardiac contractility. *J Mol Cell Cardiol* 2014;72:350-9.

55. Khairallah M, Khairallah R, Young ME, et al. Metabolic and signaling alterations in dystrophin-deficient hearts precede overt cardiomyopathy. *J Mol Cell Cardiol* 2007;43:119-29.

56. Zhang W, ten Hove M, Schneider JE, et al. Abnormal cardiac morphology, function and energy metabolism in the dystrophic mdx mouse: an MRI and MRS study. *J Mol Cell Cardiol* 2008;45:754-60.

57. Stuckey DJ, Carr CA, Camelliti P, et al. In vivo MRI characterization of progressive cardiac dysfunction in the mdx mouse model of muscular dystrophy. *PLoS One* 2012;7:e28569.

58. Bostick B, Yue Y, Duan D. Gender influences cardiac function in the mdx model of Duchenne cardiomyopathy. *Muscle Nerve* 2010;42:600-3.

59. Bell RM, Mocanu MM, Yellon DM. Retrograde heart perfusion: the Langendorff technique of isolated heart perfusion. *J Mol Cell Cardiol* 2011;50:940-50.

60. Liao R, Podesser BK, Lim CC. The continuing evolution of the Langendorff and ejecting murine heart: new advances in cardiac phenotyping. *Am J Physiol Heart Circ Physiol* 2012;303:H156-67.

61. Kaspar RW, Allen HD, Ray WC, et al. Analysis of dystrophin deletion mutations predicts age of

cardiomyopathy onset in becker muscular dystrophy. *Circ Cardiovasc Genet* 2009;2:544-51.

62. Feng J, Yan J, Buzin CH, Towbin JA, Sommer SS. Mutations in the dystrophin gene are associated with sporadic dilated cardiomyopathy. *Mol Genet Metab* 2002;77:119-26.

63. Ortiz-Lopez R, Li H, Su J, Goytia V, Towbin JA. Evidence for a dystrophin missense mutation as a cause of X-linked dilated cardiomyopathy. *Circulation* 1997;95:2434-40.

64. Singh SM, Bandi S, Shah DD, Armstrong G, Mallela KM. Missense mutation Lys18Asn in dystrophin that triggers X-linked dilated cardiomyopathy decreases protein stability, increases protein unfolding, and perturbs protein structure, but does not affect protein function. *PLoS One* 2014;9:e110439.

65. Lee TH, Eun LY, Choi JY, et al. Myocardial atrophy in children with mitochondrial disease and Duchenne muscular dystrophy. *Korean J Pediatr* 2014;57:232-9.

66. Matsuoka S, Ii K, Akita H, et al. Clinical features and cardiopulmonary function of patients with atrophic heart in Duchenne muscular dystrophy. *Jpn Heart J* 1987;28:687-94.

67. Konstam MA, Kramer DG, Patel AR, Maron MS, Udelson JE. Left ventricular remodeling in heart failure: current concepts in clinical significance and assessment. *J Am Coll Cardiol* 2011;4:98-108.

68. Silva MC, Meira ZM, Gurgel Giannetti J, et al. Myocardial delayed enhancement by magnetic resonance imaging in patients with muscular dystrophy. *J Am Coll Cardiol* 2007;49:1874-9.

69. Shirokova N, Niggli E. Cardiac phenotype of Duchenne muscular dystrophy: insights from cellular studies. *J Mol Cell Cardiol* 2013;58:217-24.

70. Nigro G, LComi LI, Politano L, Bain RJ. The incidence and evolution of cardiomyopathy in Duchenne muscular dystrophy. *Int J Cardiol* 1990;26:271-7.

71. Li Y, Zhang S, Zhang X, et al. Blunted cardiac beta-adrenergic response as an early indication of cardiac dysfunction in Duchenne muscular dystrophy. *Cardiovasc Res* 2014;103:60-71.

72. Barbin IC, Pereira JA, Bersan Rovere M, et al. Diaphragm degeneration and cardiac structure in mdx mouse: potential clinical implications for Duchenne muscular dystrophy. *J Anat* 2016;228:784-91.

73. Costas JM, Nye DJ, Henley JB, Plochocki JH. Voluntary exercise induces structural remodeling in the hearts of dystrophin-deficient mice. *Muscle Nerve* 2010;42:881-5.

74. Nakamura A, Yoshida K, Takeda S, Dohi N, Ikeda S. Progression of dystrophic features and activation of mitogen-activated protein kinases and calcineurin by physical exercise, in hearts of mdx mice. *FEBS Lett* 2002;520:18-24.

KEY WORDS cardiomyopathy, diastolic dysfunction, dystrophin, ribonucleotide reductase, recombinant adeno-associated virus vectors

APPENDIX For supplemental figures, please see the online version of this paper.